Submitted to

32nd International Conference on High Energy Physics, ICHEP04, August 16, 2004, Beijing
Abstract: **12-0185**
Parallel Session **12**

www-h1.desy.de/h1/www/publications/conf/conf_list.html

A Direct Search for Magnetic Monopoles at HERA

H1 Collaboration

Abstract

A direct search has been made for magnetic monopoles produced in e^+p collisions at a centre of mass energy of 300 GeV at HERA. The beam pipe surrounding the interaction region during 1995-1997 (integrated luminosity 60 pb^{-1}) was investigated using a SQUID magnetometer to look for stopped magnetic monopoles. No free magnetic charges were observed and charge-dependent upper limits on the cross section for the electro-production of magnetic monopoles have been set.

1 Introduction

One of the outstanding issues in modern physics is the possible existence of magnetic monopoles. Dirac showed that only one magnetic monopole is needed anywhere in the universe to explain the empirical fact of electric charge quantisation [1]. Magnetic monopoles are also predicted from field theories which unify the fundamental forces [2–5]. Furthermore, the formation of a monopole condensate provides a possible mechanism for quark confinement [6]. Nevertheless, despite a large number of searches [7] using a variety of experimental techniques no reproducible evidence has been found to support the existence of monopoles. Recent searches for monopoles produced in high energy particle collisions have been made with $p\bar{p}$ [8–10] and e^+e^- [11–16] interactions. This paper describes the first search for monopoles produced in high energy e^+p scattering at HERA.

The quantisation of the angular momentum of a system of an electron with electric charge e and a monopole with magnetic charge g leads to Dirac's celebrated charge quantisation condition $eg = nhc/4\pi$, where h is Planck's constant, c is the speed of light and n is an integer [1]. Within this approach, taking $n = 1$ sets the theoretical minimum magnetic charge which can be possessed by a particle (known as the Dirac charge g_d). However, if the elementary electric charge is considered to be held by the down quark then the minimum value of g_d will be three times larger. The value of g_d could be even higher since the application of the Dirac argument to a particle possessing both electric and magnetic charge (a so-called dyon [17, 18]) restricts the values of n to be even [17].

Monopoles are also features of current unification theories such as M-theory [2, 3] and Supersymmetric Grand Unified Theories [4, 5]. Both of these approaches tend to predict superheavy primordial monopoles with mass values in excess of 10^{15} GeV. However, in some Grand Unified scenarios values of monopole mass as low as 10^4 GeV [20–22] are allowed. Light monopoles are also predicted in other approaches [23–26] and postulates on values of the classical radius of a monopole lead to estimates of mass of $\mathcal{O}(10)$ GeV [19].

Since the value of the coupling constant of a photon to a monopole ($\alpha_m \approx 34n^2$) is substantially larger than for a photon-electron interaction ($\alpha_e \approx 1/137$) perturbative field theory cannot be reliably used to calculate the rates of monopole processes. The large coupling also implies that ionisation energy losses will be typically several orders of magnitude greater for monopoles than for minimum ionising electrically charged particles [27–29].

Direct experimental searches using a variety of tracking devices to detect the passage of highly ionising particles with monopole properties have been made [7]. Monopoles which stop in matter such as material at accelerators [9] and lunar rock [30–32] and monopoles in cosmic rays [33] have been sought via the induction of a persistent current within a superconducting loop [30, 34], the method adopted here. Measurements of multi-photon production [10, 16] allow indirect searches to be made. However, the inapplicability of perturbative field theory renders these limits unreliable [35, 36].

For the direct search reported here we use the fact that heavily ionising magnetic monopoles produced in e^+p collisions may stop in the beam pipe surrounding the H1 interaction point at HERA. The binding energy of monopoles in the material is expected to be large [36] and so they should remain permanently trapped providing they are stable. The beam pipe has been measured using a SQUID magnetometer with a sensitivity of $0.2g_d$ after a single traversal of a sample to look for the persistent currents from such trapped monopoles.

2 The Experimental Method

A section of the aluminium beam pipe used in 1996-1998 of length 58 cm centred on the interaction point was cut into 15 longitudinal strips. The strips were passed through the 2G Enterprises type 760 magnetometer [38] at the Southampton Oceanography Centre. This is a warm bore device with high sensitivity and low noise level. The strips were passed axially once through the magnetometer in steps, pausing for 1 second after each step, to look for a persistent change in current in the coil oriented perpendicular to the direction of the traversal. Such a change in the final current would be induced by the passage of a monopole whereas dipole impurities cause a current which returns to zero after the traversal of the strip. The reading for each strip was repeated several times. This allowed the reproducibility of the results to be studied so that random flux jumps and base line drifts could be identified. Any real monopole in the pipe would give a consistent and reproducible current step.

A long (0.7 m length) solenoid was used to assess the sensitivity of the SQUID Magnetometer to a monopole. The magnetic field outside of the ends of a long solenoid is similar to that produced by a monopole. A solenoid can thus be considered as possessing two oppositely charged "pseudopoles" of pole strength $g_d = niS/3.3\ 10^{-9}$ in units of the Dirac charge. Here n is the number of turns per metre length, i is the current and S is the cross sectional area of the coil and the factor $3.3\ 10^{-9}$ Am is the Dirac charge. Hence the current and radius of the solenoid can be chosen to mimic the desired pole strength.[1] To calibrate the solenoid was stepped through the magnetometer. Data were taken with different currents subtracting the measurements with zero current to correct for the dipole impurities in it. The measured increase in current in the magnetometer following the passage of one end of the solenoid is shown in Fig. 1 as a function of pseudopole strength (in units of g_d).

To simulate trapped monopole behaviour the long calibration solenoid was placed along a strip and passed through the magnetometer. Only one end of the calibration solenoid was allowed to traverse the magnetometer hence simulating the passage of a monopole in the strip. Fig. 2 shows the absolute value of the measured magnetometer current as the strip alone was stepped through and when pseudopoles of values g_d and $-g_d$ were attached. The large structure at the centre comes from the dipole impurities in the aluminium. The final persistent magnetometer current is consistent with the value expected (shown as the the dashed lines). Shown inset, on a linear scale, is the value of the measured current as the strip leaves the magnetometer pickup coil. The values of current for g_d and $-g_d$ pseudopoles are approximately equal and opposite and at the value expected from the calibration performed purely with the solenoid. The deviations are due to small dipole impurities in the former of the copper coil.

Fig. 2 illustrates that if a monopole of strength greater than a fraction of a Dirac monopole had been trapped by the beam pipe its persistent current would have been seen.

3 Results

The data were taken in two separate runs. In the first run 13 of the strips were passed through the magnetometer once for each strip. Two of the strips showed persistent currents of a value

[1] A study integrating the Biot Savart Law for the magnetic field outside the dimensions of the magnetometer coil shows that this simple formula is accurate to $\sim \pm 3\%$.

expected from the passage of a magnetic charge of strength 1 g_d each with a sign equivalent to a North seeking pole i.e. one that is accelerated in the $+z$ direction by the H1 magnetic field of 1.15 Tesla. The strips were then remeasured several times during a second run. In this run none of the strips showed any persistent current after traversal through the magnetometer. It was therefore assumed that the two observed persistent currents during the first run had been caused by random flux jumps (which occurred during about 10% of the readings). The binding energy of monopoles in solids is thought to be hundreds of kilovolts [36] compared to those of atoms which are at the eV level. Nevertheless the strips were carefully stored between the two runs to avoid dislodging any monopole present. They had also been carefully stored and not been subject to heat or strong magnetising or demagnetising fields after removal from the H1 apparatus.

Fig 3 shows a summary of all the readings from the second run. The values of the monopole strength on the vertical axis were computed by taking the difference between the first reading as the moving table entered the magnetometer (before the strip entered) and the last reading which came 40 cm after the strip left the magnetometer coil. Strips 1 and 3 show some activity in one reading each, at the level of 0.2 g_d. This activity was compatible with zero on all other passes and it was compatible with zero if the penultimate reading is used for the exit current rather than the last reading. It is concluded therefore that this reading is spurious possibly caused by something such as a speck of dust falling on the table. The overall root mean square deviation of the readings was 0.07 g_d (shown as the dashed lines in Fig. 3). This illustrates the remarkable improvements in SQUID technology since previous measurements using this technique (e.g. see [30–32]) where many traversals were needed to achieve noise levels approaching this value compared to the single traverals reported here.

It is concluded therefore that no consistently repeatable monopole signal was seen in any of the beam pipe strips examined. From Fig. 3 it can be seen that the magnetometer was sensitive to monopole strengths above about 0.2 g_d.

4 Upper Limits on the measured Cross Sections

To derive an upper limit on the measured cross section it is necessary to compute the acceptance, i.e. the fraction of the monopoles produced which would have been detected. A model of the production process is therefore needed. A simple model was used here to compute the acceptance by Monte Carlo technique. This model assumed that a monopole(M)-antimonopole ($\bar{M}$) pair are produced by the photoproduction process $\gamma p \rightarrow M\bar{M}p$ through a $\gamma - \gamma$ interaction with a photon radiated from each of the electron and proton. The model depends on perturbation theory to compute the cross sections which are therefore unreliable as noted previously. However, it is assumed that computations of the acceptance will be roughly correct since these mainly depend on the kinematics. Events were generated according to this model using the programme CompHep [39] and the final state particles tracked through the H1 magnetic field (B=1.15 Tesla) and the beam pipe to determine the fraction of the monopoles which stop.

Monopoles have a parabolic trajectory in a magnetic field of the form

$$z - z_v = 0.5 \frac{gBr^2}{ep_T \beta_T} + \frac{r}{\tan\theta_0} \quad (1)$$

where z_v is the z coordinate of the vertex and z is the coordinate of a point on the trajectory at distance r from the proton beam (taken to define the $+z$ axis). The transverse momentum and tranverse velocity of the monopole are p_T and β_T, respectively. The electric charge is e and θ_0 is the initial angle of the monopole to the proton beam direction. In this equation g is negative(positive) for South(North) poles which decelerate (accelerate) in the $+z$ direction in the H1 magnetic field. The geometric acceptance is the fraction of the monopoles which traverse the beam pipe in the cut length. The total acceptance is this fraction times the fraction which stop in the pipe. The range of monopoles in aluminium was computed by integrating the stopping power, dE/dx, given in [28] adjusted for the electron density in aluminium. Fig. 4 shows the computed range (normalised to mass) for monopoles of strength 1 g_d versus $p/m = \beta\gamma$ where p and m are the momentum and mass of the monopole, respectively, and β, γ are its velocity factors. The stopping power was computed in [27–29] by classically considering the long range monopole interactions with atomic electrons.

Fig 5 shows the total efficiency for stopping a monopole in the section of beampipe under investigation. This was computed from the model for magnetic charges of 1,2,3 and 6 g_d using the range calculations given in the previous figure divided by the square of the monopole charge considered. The mass values extend out to about 120 GeV albeit with lower efficiencies in these regions since heavier monopoles are preferentially produced in the foward region due to the phase space limitations caused by the asymmetry in the momenta of the colliding beams at HERA. Since the value of the ionisation energy loss increases as the square of the monopole charge this similarly leads to a rapid increase of stopping efficiency. For monopoles of charge $6g_d$ and above the efficiency becomes limited by the geometric acceptance of the beam-pipe section considered.

The upper limit on the cross section for monopole-antimonopole pair production was derived as follows. Observation of zero monopole candidates means that we must have had less than 3 events at 95 $\%$ confidence level. It is assumed that the flux of monopoles is not so high that there is an equal number of pairs in each strip to cancel the signal. The pipe was exposed to a total luminosity of 60 pb^{-1}. A total of 13 strips have been analysed to date corresponding to 75$\%$ of the mass of the pipe after cutting. [2] The acceptance was computed from the model described above. Fig. 6 shows the upper limit on the cross section at 95$\%$ confidence for monopoles of strength 1,2, 3 and 6 g_d.

Other experiments have also produced limits on monopole production cross-sections for different masses and charges [8, 9, 11–15]. However, owing to the lack of a reliable field theory for monopole production different model assumptions were made in their derivations. Furthermore, although a universal production mechanism for monopole production can be postulated, comparisons of cross-section limits in processes as diverse as e^+p, $p\bar{p}$ and e^+e^- should be treated with care. Nevertheless, the regions of charge and mass which are excluded are largely determined by acceptance effects.

Fig. 7 shows the cross-section upper limit as a function of mass for monopoles of charge g_d produced in e^+p scattering in this analysis, $p\bar{p}$ interactions at the Tevatron [8, 9] and e^+e^- interactions at LEP [15],Tristan [13] and Petra [11]. The regions which are excluded are denoted. The results from H1 extend over a larger mass region than in e^+e^- although these latter results

[2]The remaining 2 strips were cut into smaller pieces which will be studied in the future.

exclude lower values of the cross-section. The results from the Tevatron extend to larger values of mass and cover lower cross-section values than H1. However, the most recent of these results [9] relies on assumptions of the stability of monopole binding which are far more stringent than ours[3].

The same curves are shown in Fig. 8 with an additional limit derived from studies of lunar soil [32]. Here, the interactions of the cosmic rays with the surface of the moon over 500 Myears is used to derive an upper limit for monopole pair production for pn scattering. This relies on a number of assumptions including the stability of energy distributions of cosmic rays over a large period of time and of the churning rate of the lunar surface. Nevertheless it provides the best limit.

Fig. 9 shows the same curves as in Fig. 7 but for monopoles of charge $2g_d$. Again the H1 masslimit extends beyond that from e^+e^- results but below that from $p\bar{p}$ interactions. However, the H1 results are able to exclude lower values of cross-section than either experiment.

Limits from monopoles of charge $3g_d$ are shown in Fig. 10. At this charge it is seen that e^+e^- results are only able to exclude low values of mass (<10 GeV). Similar conclusions can be drawn from the upper limits for monopoles of charge $6g_d$ which are shown in Figs. 11.

5 Conclusions

A search for magnetic monopoles produced in e^+p collisions at HERA at a centre of mass energy of $\sqrt{s} = 300$ GeV has been made for the first time. Monopoles trapped in the beam pipe were directly sought by examining it with a sensitive SQUID magnetometer. No reproducible signal was observed allowing upper limits on the monopole pair production cross section to be set for monopoles with values of charges and masses from 1 to 6 g_d and up to about 150 GeV, respectively.

The search is sensitive to a greater range of monopole mass and charge than in studies of e^+e^- interactions. Limits from $p\bar{p}$ interactions exclude larger values of mass albeit with more model assumptions than used here.

In the future we hope to extend the mass range of the limits and improve the sensitivity by examining a further length of the beam pipe.

References

[1] P.A.M. Dirac, Proc. Roy. Soc. **133** (60) 1931, Phys. Rev. **74** (817) 1948;
Alternative derivations of the Dirac quantisation condition can be found in
J.D. Jackson, *Classical Electrodynamics*, 3^{rd} edition (John Wiley, New York, 1999);
M. Kaku, *Quantum Field Theory, a Modern Introduction*, 1^{st} edition (Oxford University Press, New York, 1993).

[3] In order to attempt to reduce the dipole moment background the samples were degaussed and heat treated [40] procedures which we have avoided here due to the unknown chemistry of magnetic monopoles.

[2] R.D. Sorkin, Phys. Rev. Lett. **51** (87) 1983;
D.J. Gross and M. Perry, Nucl. Phys. **B 226** (29) 1983.

[3] E. Bergshoeff, E. Eyras, Y. Lozanos, Phys. Lett. **B 430** (77) 1998.

[4] G. 't Hooft, Nucl. Phys. **B 79** (276) 1974;
A. Polyakov, Pi'sma. Eksp. Teor. Fiz. **20** (430) 1974, JETP Lett **20** (1994) 1974.

[5] H. Mikakata, Phys. Lett. **B 155** (352) 1985;
J.L. Lopez, Rep. Prog. Phys. **59** (819) 1996.

[6] Y. Nambu, Phys. Rev. **D 10** (4262) 1974;
S. Mandelstam, Phys. Rev. **C 23** (245) 1976;
A. Polyakov, Nucl. Phys. **B 120** (429) 1977;
G. 't Hooft, Nucl. Phys. **B 190** (455) 1981.

[7] D.E. Groom *et al.*, (Particle Data Group), Eur. Phys. J. **C 15** (1) 2000.

[8] M. Bertani *et al.*, Eur. Phys. Lett. **12** (613) 1990.

[9] G.R. Kalbfleisch *et al.*, Phys. Rev. Lett. **85** (5292) 2000.

[10] B. Abbot *et al.*, Phys. Rev. Lett. **81** (524) 1998.

[11] P. Musset, M. Price and E. Lohrmann Phys. Lett. **B 128** (333) 1983.

[12] R. Braunschweig *et al.*, Z. Phys. **C 38** (543) 1988.

[13] K. Kinoshita *et al.*, Phys. Lett. **B 228** (543) 1989.

[14] K. Kinoshita *et al.*, Phys. Rev. **D 46** (881) 1992.

[15] J.L. Pinfold *et al.*, Phys. Lett. **B 316** (407) 1993.

[16] M. Acciari *et al.*, Phys. Lett. **B 345** (609) 1995.

[17] J. Schwinger, Phys. Rev. **144** (1087) 1966, **173** (1536) (1968), Science **165**, (3895) 1969.

[18] P.C.M. Yock, Int. J. Theor. Phys. **2** (247) 1969;
A. De Rujula, R.C. Giles and R.L. Jaffe, Phys. Rev. **D 17** (285) 1978;
D. Fryberger, Hadronic J. **4** (1844) 1981.

[19] H.V. Klapdor-Kleingrothaus, K. Zuber, *Particle Astrophysics*, 1^{st} edition (The Institute of Physics, UK, 1999).

[20] T.G. Rizzo and G. Senjanovic, Phys. Rev. Lett. **46** (1315) 1981, Phys. Rev. **D 24** (704) 1981, Phys. Rev. **D 25** (235) 1982 (E: **D25** (1982)).

[21] J. Preskill Ann. Rev. Nucl. Part. Sci. **34** (461) 1984.

[22] E.J. Weinberg, Nucl. Phys. **B 236** (90) 1984.

[23] T. Kirkman and C. Zachos, Phys. Rev. **D 24** (999) 1981.

[24] Yisong Yang, Proc. Roy. Soc. **A454**, 155 (1998), *Solitons in Field Theory and Nonlinear Analysis* (Springer Monographs in Mathematics, 2001);
Y.M. Cho, hep-th/0210298.

[25] F.A. Bais, W. Troost, Nucl. Phys. **B**178 **125** (1981) .

[26] T. Banks, M. Dine, H. Dystra, W. Fischler, Phys. Lett. **B 212** (45) 1988

[27] S.P. Ahlen,Phys. Rev. **D 14** (2935) 1976.

[28] S.P. Ahlen,Phys. Rev. **D 17** (229) 1978.

[29] S.P. Ahlen, K. Kinoshita, Phys. Rev. **D 26** (2347) 1982.

[30] L.W. Alvarez *et al.*, Science **167** 701 1970.

[31] P.H. Ebehard *et al.*, Phys. Rev. **D 4** (3260) 1971.

[32] R.R. Ross *at al.*, Phys. Rev. **D 8** (698) 1973.

[33] See, for example, B. Cabrera, Phys. Rev. Lett. **48** (1378) 1982;
A.D. Caplin *et al.*, Nature **321** 402 (1986).

[34] D.J Griffiths, *Introduction to Electrodynamics*, 3^{rd} edition, (Prentice Hall, New Jersey, 1999).

[35] A. De Rujula, Nucl. Phys. **B 435** (257) 1995.

[36] L. Gamberg, G. Kalbfleisch and K. Milton, hep-ph/9805365.

[37] R. Weeks *et al.*, Geophys. J. Int., **114**, 651, 1993.

[38] URL:http://www.2genterprises.com.

[39] CompHEP - A. Pukhov et al arXiv:hep-ph/9908288.

[40] G.R. Kalbfleisch, private communication.

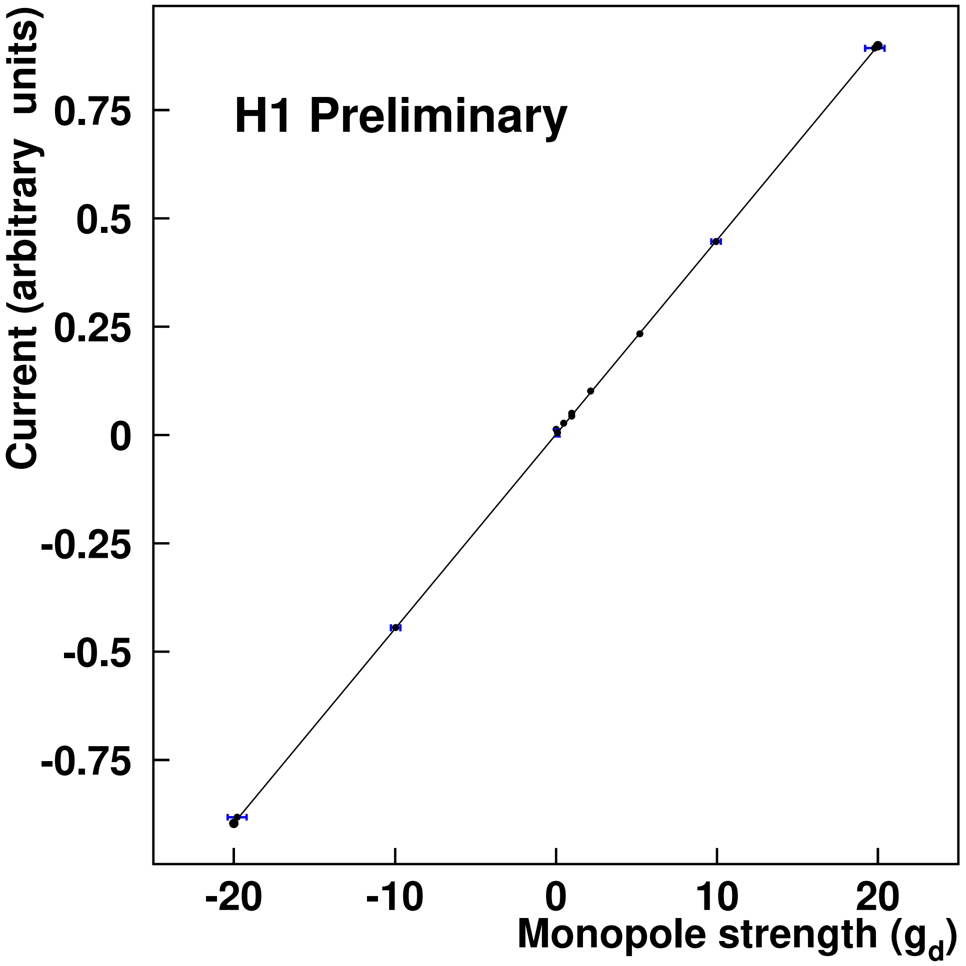

Figure 1: The magnitude of the observed steps versus pole strength for each calibration coil current (the conversion accuracy is $\pm 3\%$ point to point with a further overall normalisation accuracy of $\pm 3\%$ due to the uncertainty in the coil diameter). The solid line shows a linear fit to the data which gives the calibration constant to be 0.045 units per unit Dirac monopole charge.

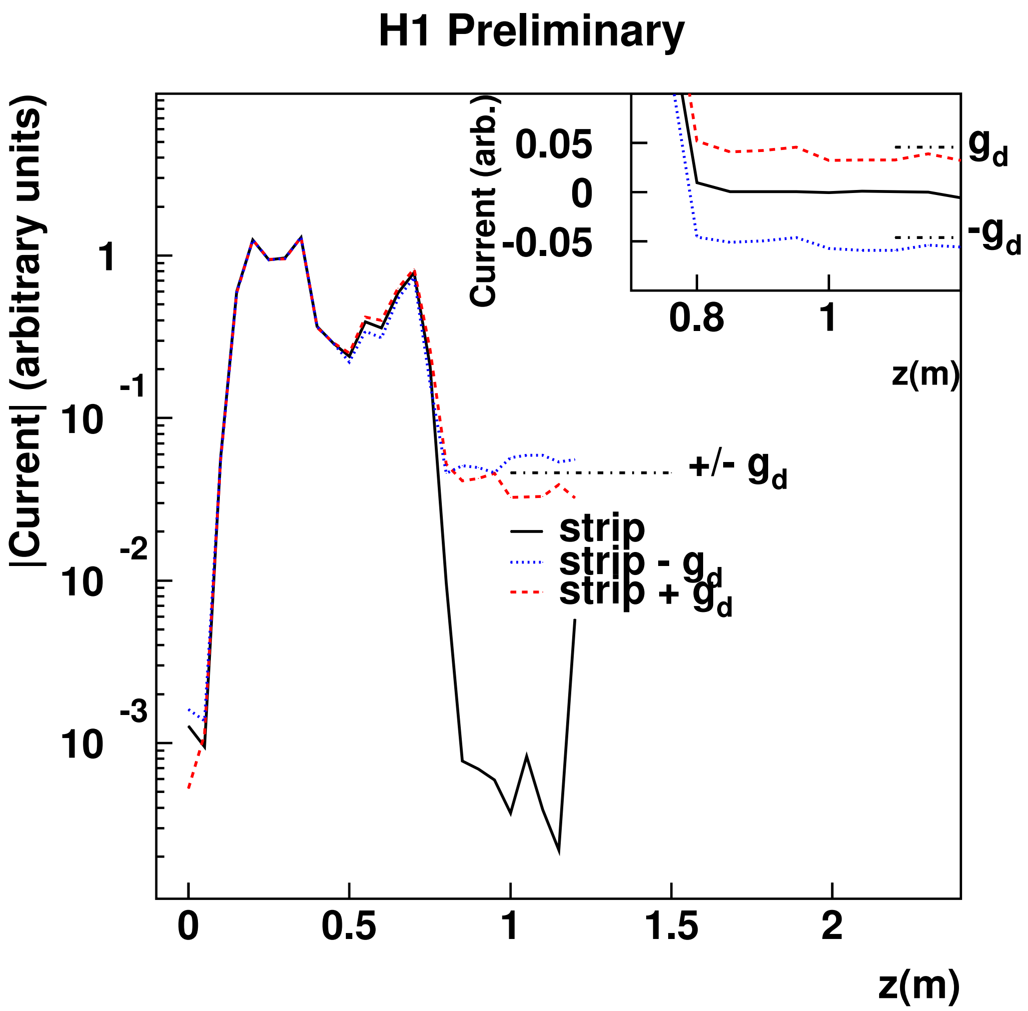

Figure 2: The absolute value of the magnetometer current on a logarithmic scale versus step position (z) from a strip with a solenoid mounted on it. The solenoid current was chosen to simulate a pole strength of 1 g_d (red dashed curve) and -1 g_d (blue dotted curve). The solid black curve shows the readings with the solenoid removed. The inset shows the signed measurements of the same currents on a linear scale.

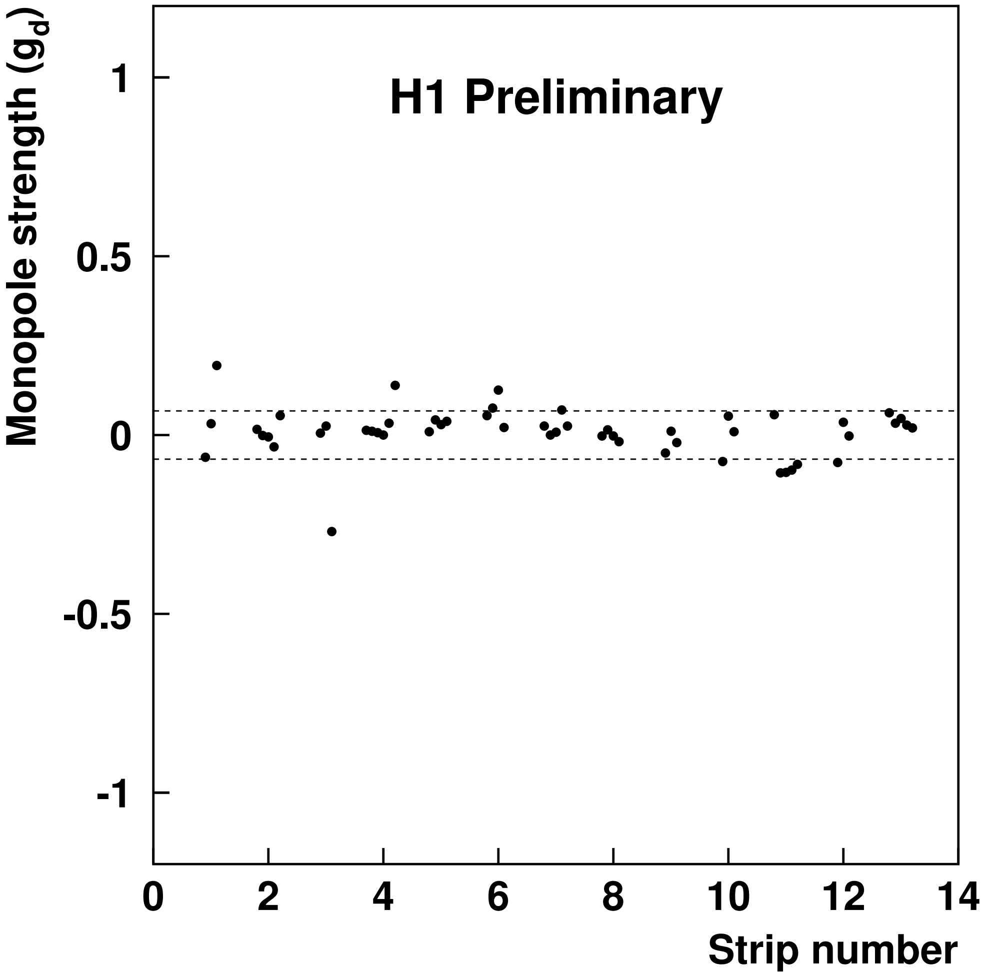

Figure 3: The observed persistent currents in each strip against strip number. The different measurements for the same strip are staggered in strip number for visibility. The dashed lines show the root mean square deviation of the readings.

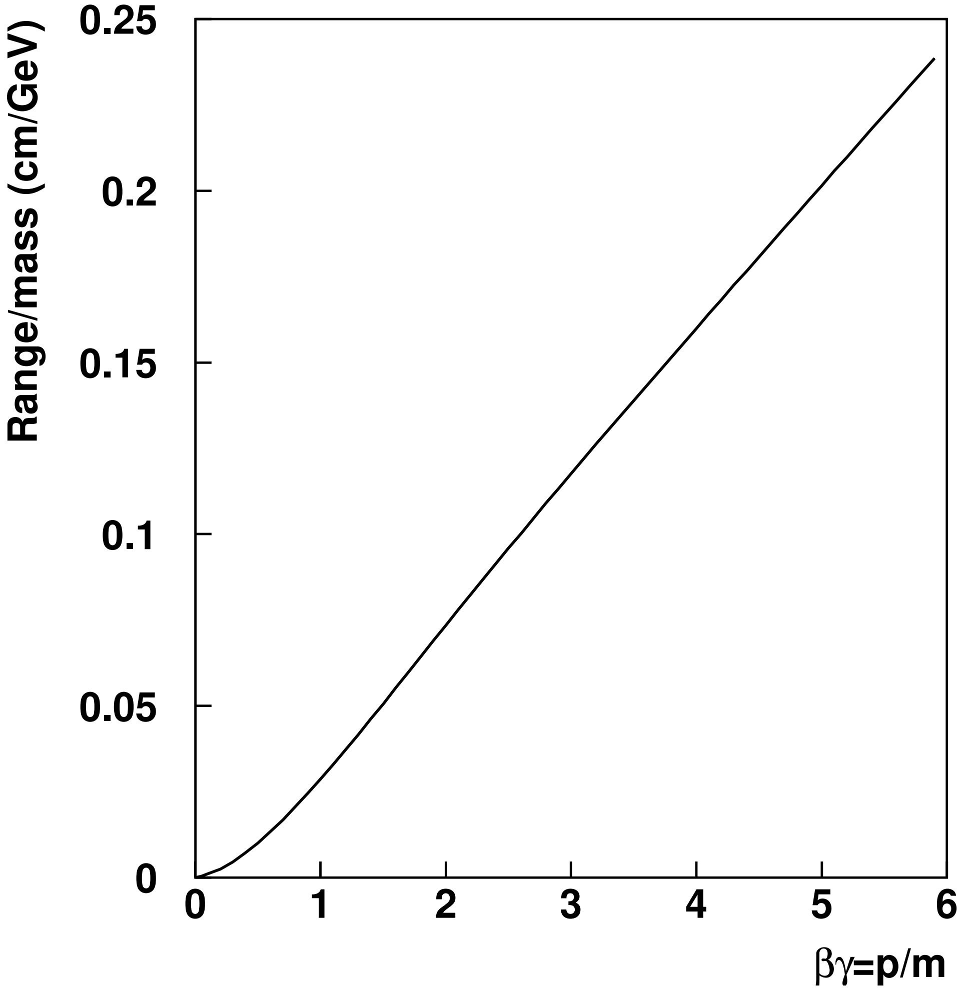

Figure 4: Range/mass of a monopole in aluminium versus $\beta\gamma$ calculated from the stopping power, dE/dx, in Fig 1 of [28] adjusted to the electron density in aluminium.

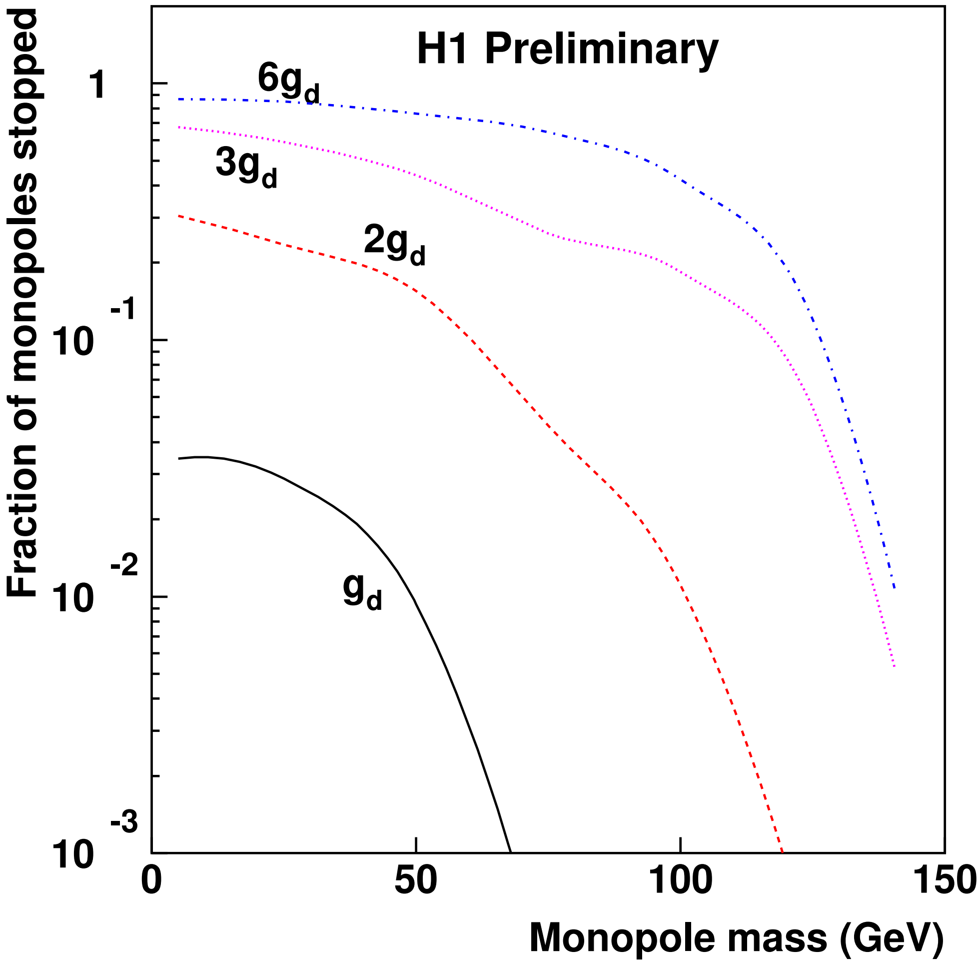

Figure 5: The total efficiency for stopping a monopole of strength g_d, $2g_d$, $3g_d$ and $6g_d$.

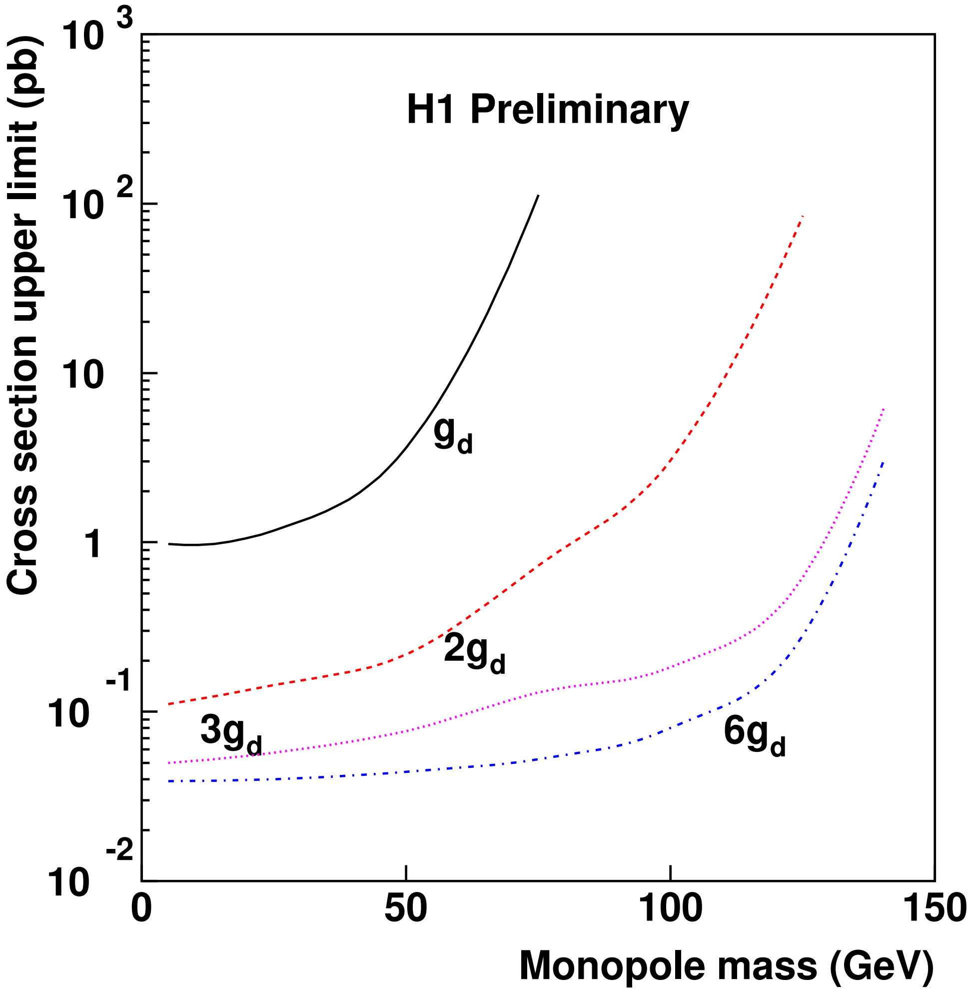

Figure 6: Upper limits on the cross section for monopole-antimonopole pair production as a function of monopole mass for monopoles of strength g_d, $2g_d$, $3g_d$ and $6g_d$.

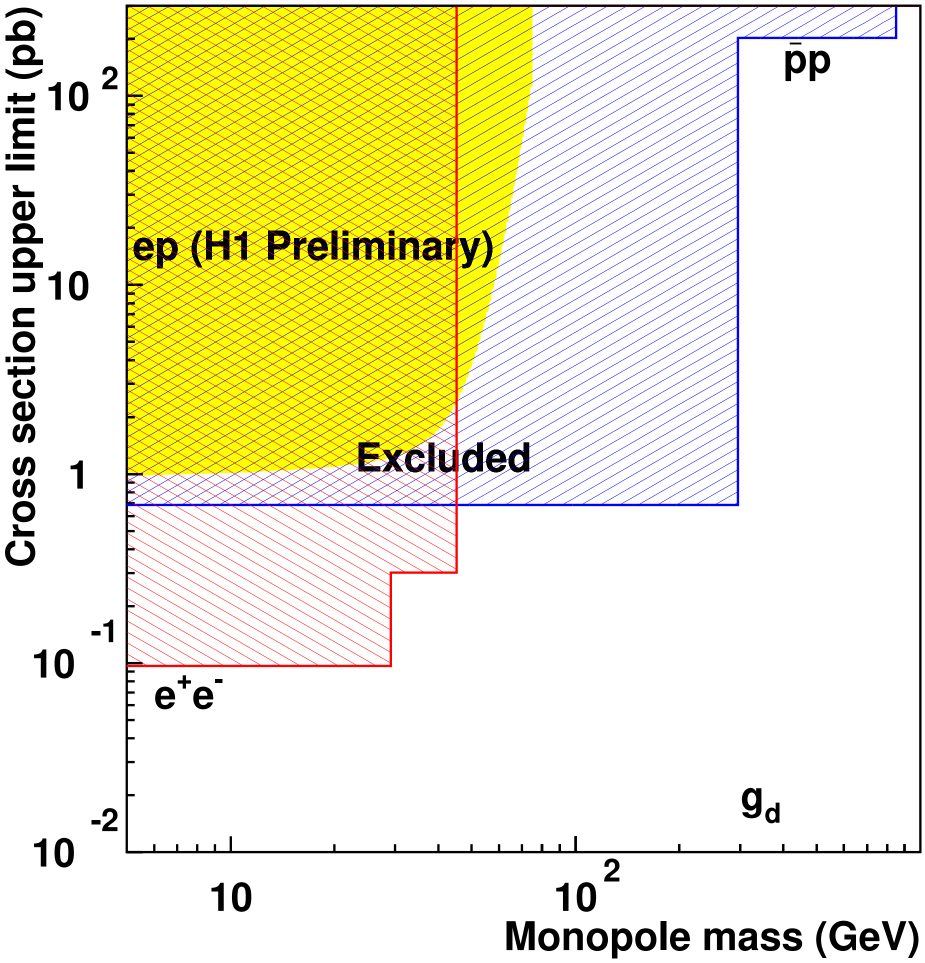

Figure 7: Upper limits on the cross section for monopole-antimonopole pair production as a function of monopole mass for monopoles of strength g_d compared with limits obtained in $p\bar{p}$ and e^+e^- interactions.

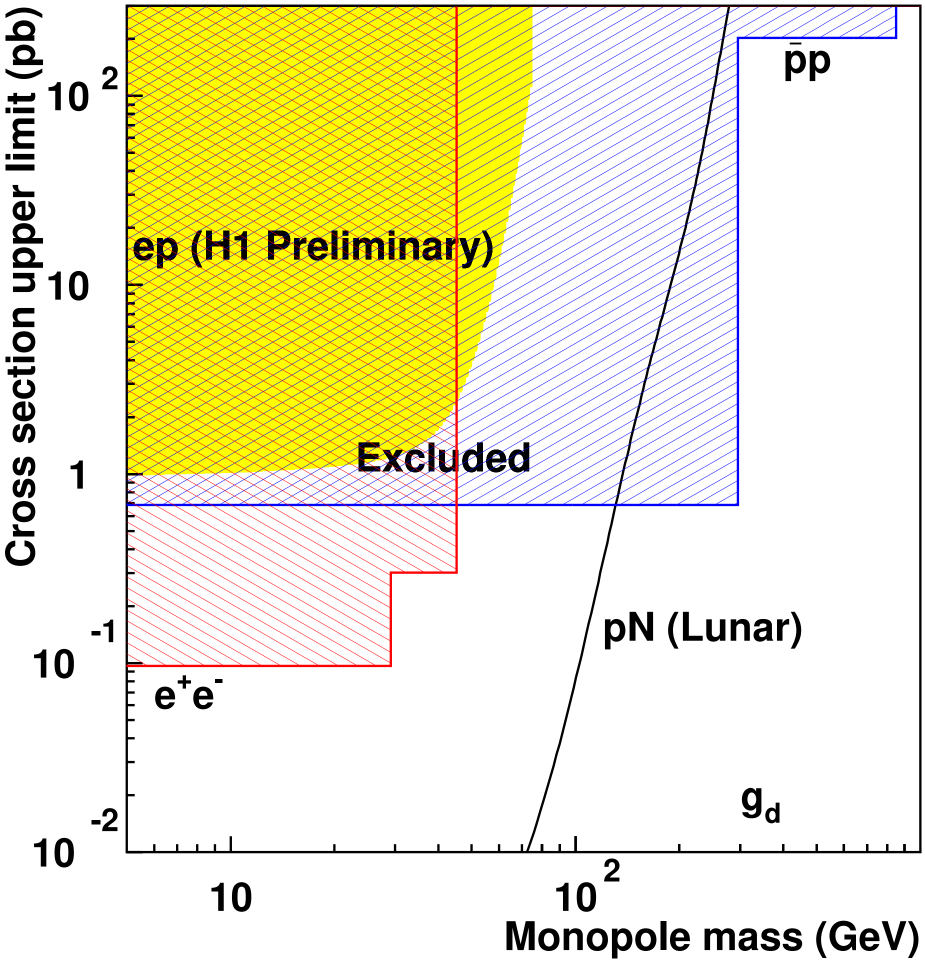

Figure 8: Upper limits on the cross section for monopole-antimonopole pair production as a function of monopole mass for monopoles of strength g_d compared with limits obtained in $p\bar{p}$ and e^+e^- interactions and from lunar rock.

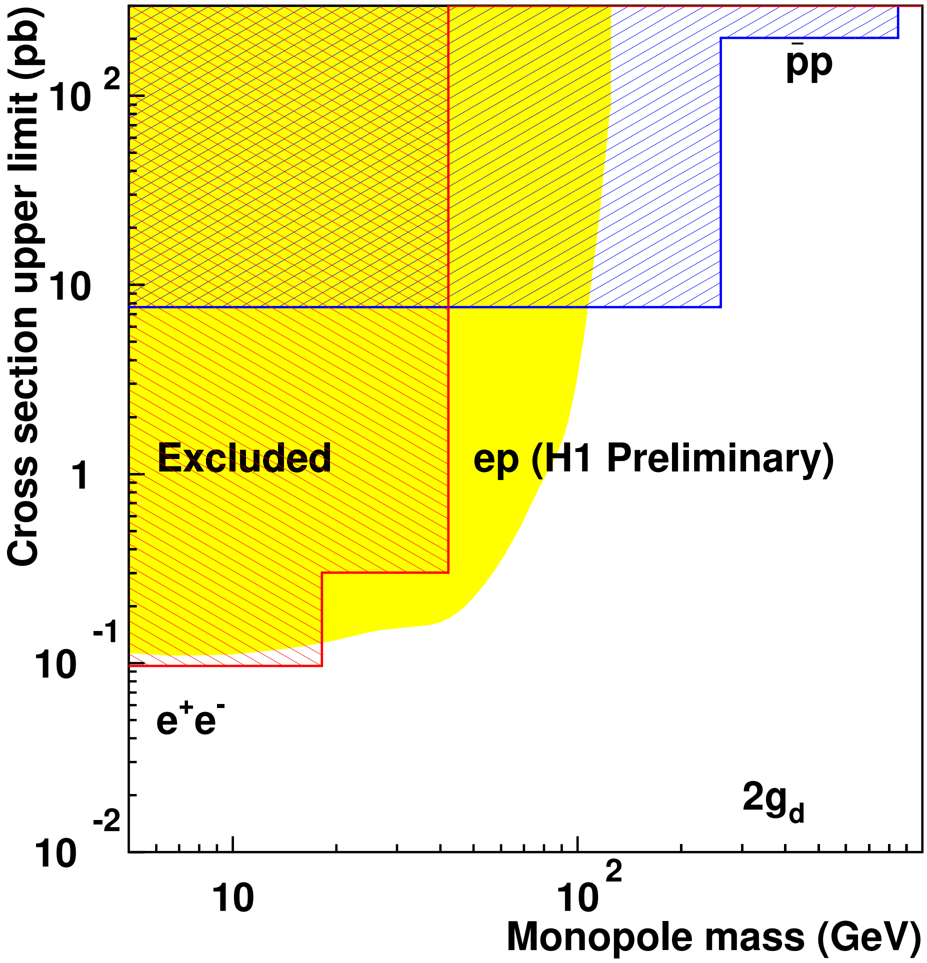

Figure 9: Upper limits on the cross section for monopole-antimonopole pair production as a function of monopole mass for monopoles of strength $2g_d$ compared with limits obtained in $p\bar{p}$ and e^+e^- interactions.

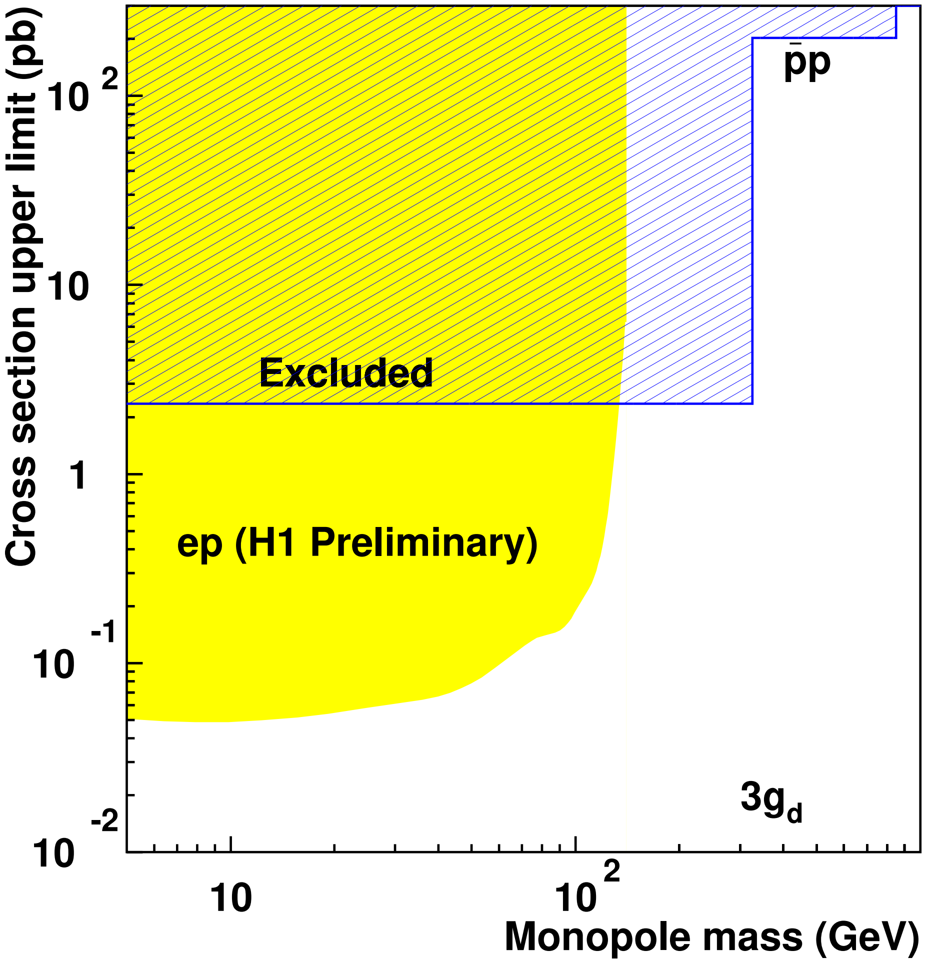

Figure 10: Upper limits on the cross section for monopole-antimonopole pair production as a function of monopole mass for monopoles of strength $3g_d$ compared with limits obtained in $p\bar{p}$ and e^+e^- interactions.

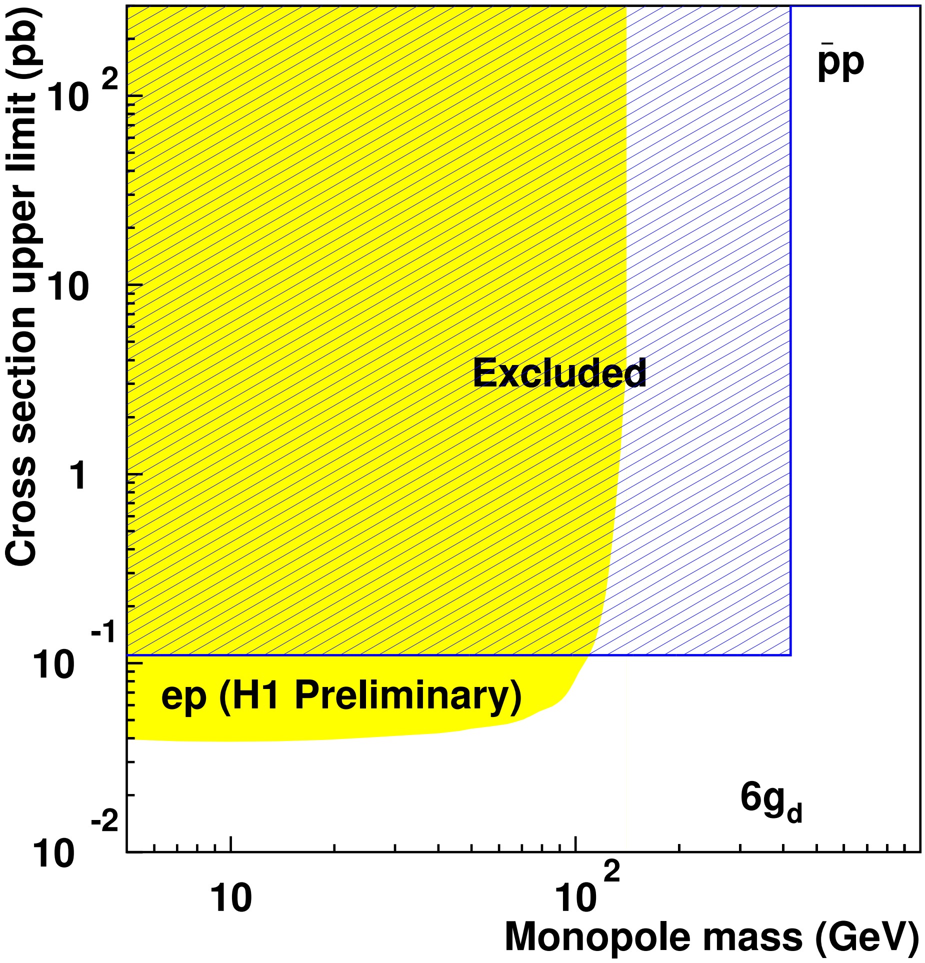

Figure 11: Upper limits on the cross section for monopole-antimonopole pair production as a function of monopole mass for monopoles of strength $6g_d$ compared with limits obtained in $p\bar{p}$ and e^+e^- interactions.